Standard and non-standard neutrino properties

J. W. F. Valle[a] *

[a]Instituto de Física Corpuscular – C.S.I.C./Universitat de València
Edificio Institutos de Paterna, Apt 22085, E–46071 València, Spain

I review the interpretation of solar and atmospheric neutrino data in terms neutrino oscillations and describe some ways to account for the required neutrino masses and mixing angles from first principles, both within top-down and bottom-up approaches. I also discuss non-oscillation phenomena such as $\beta\beta_{0\nu}$ which may probe the absolute scale of neutrino mass, and also reveal its Majorana nature. I note that leptonic CP violation induced by "Majorana" phases drop from oscillations but play a role in the leptogenesis scenario for the baryon asymmetry of the Universe. Direct tests of leptonic CP violation in oscillation experiments, such as neutrino factories, will be a tough challenge, due to the hierarchical neutrino mass splittings and the smallness of θ_{13} indicated by reactors. The large solar mixing angle θ_{12} offers a way to probe otherwise inaccessible features of supernova physics. Finally, I note that in low-scale models of neutrino mass, one may probe `all` mixing angles, including the atmospheric θ_{23}, at high energy accelerator experiments such as the LHC or NLC. A neat example is supersymmetry with bilinear breaking of R parity, where the LSP decay branching ratios are directly correlated to the neutrino mixing angles. I also discuss non-oscillation solutions to the solar neutrino problem in terms of spin-flavor precession and non-standard neutrino interactions, which will be crucially tested at KamLAND.

1. SOLAR NEUTRINOS

Solar neutrinos have now been detected with the geochemical method [1] via the $\nu_e + {}^{37}\mathrm{Cl} \to {}^{37}\mathrm{Ar} + e^-$ reaction at Homestake, and via the $\nu_e + {}^{71}\mathrm{Ga} \to {}^{71}\mathrm{Ge} + e^-$ reaction at the Gallex, Sage and GNO experiments. Direct detection with Cherenkov techniques using $\nu_e e$ scattering on water at Super-K [2], and heavy water at SNO [3] have given a robust confirmation that the number of solar neutrinos detected in underground experiments is less than expected from theories of energy generation in the sun [4]. Especially relevant is the sensitivity of the SNO experiment to the neutral current (NC).

Altogether these experiments provide a solid evidence for solar neutrino conversions and, as a result, imply that an extension of the Standard Model of particle physics in the lepton sector is needed.

Although not yet unique, the most popular explanation of solar neutrino experiments is provided by the neutrino oscillations hypothesis. Present data indicate that the mixing angle is large [5, 6], the best description being given by the LMA MSW-type [7] solution, already hinted previously from the flat Super-K recoil electron spectra [8]. The absence of a clear hint for day-night or seasonal variation in the solar neutrino signal places important restrictions on neutrino parameters.

In ref. [5] the solar neutrino data, including the latest 1496–day data and the SNO NC result have been analysed in the general framework of mixed active-sterile neutrino oscillations, where the electron neutrino produced in the sun converts to a combination of an active non-electron neutrino ν_x (a combination of ν_μ and ν_τ) and a sterile neutrino ν_s : $\nu_e \to \sqrt{1-\eta_s}\,\nu_x + \sqrt{\eta_s}\,\nu_s$. The setting for such scenarios are four-neutrino mass schemes [9] which try to accommodate the solar and atmospheric mass-splittings with the hint for short baseline oscillations from LSND [10] indicating a large Δm^2. The parameter η_s with $0 \le \eta_s \le 1$ describes the fraction of sterile neutrinos taking part in the solar oscillations.

*Work supported by Spanish grant PB98-0693, by the European Commission RTN network HPRN-CT-2000-00148, by the European Science Foundation network grant N. 86

In Fig. 1 we display the regions of solar neutrino oscillation parameters for 3 d.o.f. with respect to the global minimum, for the standard case of active oscillations, $\eta_s = 0$, as well as for $\eta_s = 0.2$ and $\eta_s = 0.5$. The first thing to notice is the impact of the SNO NC, spectral, and day/night data in improving the determination of the oscillation parameters: the shaded regions after their inclusion are much smaller than the hollow regions delimited by the corresponding $\mathrm{SNO}^{\mathrm{rate}}_{\mathrm{CC}}$ confidence contours. Especially important is the full $\mathrm{SNO}^{\mathrm{SP,DN}}_{\mathrm{CC,NC}}$ information in closing the LMA region from above: values of $\Delta m^2_{\mathrm{SOL}} > 10^{-3}$ eV^2 appear only at 3σ. Previously solar data on their own could not close the LMA region, only the inclusion of reactor data [11] probed the upper part of the LMA region [12]. Furthermore, the complete $\mathrm{SNO}^{\mathrm{SP,DN}}_{\mathrm{CC,NC}}$ information is important for excluding `maximal` solar mixing in the LMA region. At 3σ we find the upper bound (1 d.o.f.):

$$\mathrm{LMA}: \quad \tan^2\theta_{\mathrm{SOL}} \leq 0.83\,. \tag{1}$$

In order to compare the allowed regions in Fig. 1 with others [6], one must note that our C.L. regions correspond to the 3 d.o.f. : $\tan^2\theta_{\mathrm{SOL}}$, $\Delta m^2_{\mathrm{SOL}}$ and η_s. Therefore at a given C.L. our regions are larger than the usual regions for 2 d.o.f., because we also constrain the parameter η_s. Our global best fit point occurs for active oscillations with

$$\tan^2\theta_{\mathrm{SOL}} = 0.44\,, \quad \Delta m^2_{\mathrm{SOL}} = 6.6\times 10^{-5}\ \mathrm{eV}^2 \tag{2}$$

A concise way to illustrate the above results is displayed in Fig. 2. We give the profiles of $\Delta\chi^2_{\mathrm{SOL}}$ as a function of $\Delta m^2_{\mathrm{SOL}}$ (left) as well as $\tan^2\theta_{\mathrm{SOL}}$ (right), by minimizing with respect to the undisplayed oscillation parameters, for the fixed values of $\eta_s = 0,\ 0.5,\ 1$. By comparing top and bottom panels one can clearly see the impact of the full $\mathrm{SNO}^{\mathrm{SP,DN}}_{\mathrm{CC,NC}}$ sample in leading to the relative worsening of all non-LMA solutions with respect to the preferred active LMA solution. One sees also how the preferred LMA status survives in the presence of a small sterile admixture characterized by η_s (also seen in Figs. 1 and 3). Increasing η_s leads to a deterioration of all oscillation solutions.

It is also instructive to display the profile of $\Delta\chi^2_{\mathrm{SOL}}$ as a function of $0 \leq \eta_s \leq 1$, irrespective

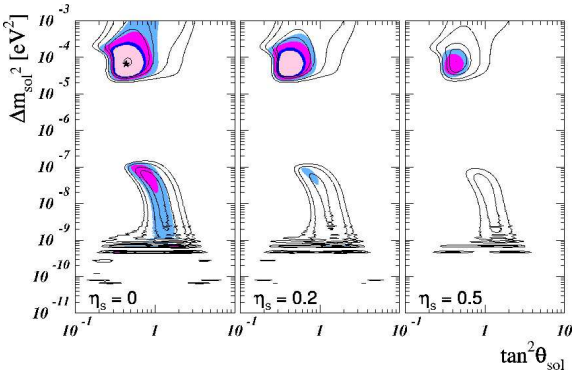

Figure 1. Allowed $\tan^2\theta_{\mathrm{SOL}}$ and $\Delta m^2_{\mathrm{SOL}}$ regions for $\eta_s = 0$ (active oscillations), $\eta_s = 0.2$ and $\eta_s = 0.5$. The lines and shaded regions correspond to the $\mathrm{SNO}^{\mathrm{rate}}_{\mathrm{CC}}$ and $\mathrm{SNO}^{\mathrm{SP,DN}}_{\mathrm{CC,NC}}$ analyses, respectively, as defined in Ref. [5]. The 90%, 95%, 99% C.L. and 3σ contours are for 3 d.o.f..

of the detailed values of the solar neutrino oscillation parameters $\Delta m^2_{\mathrm{SOL}}$ and θ_{SOL}, as shown in Fig. 3. One can see that there is a crossing between the LMA and quasi–vacuum–oscillations (QVO) solutions. This implies that the best pure–sterile description lies in the QVO regime. However, in the global analysis pure sterile oscillations with $\eta_s = 1$ are highly disfavored. We find a χ^2-difference between pure active and sterile of $\Delta\chi^2_{\mathrm{s-a}} = 32.9$ if we restrict to the LMA solution, or $\Delta\chi^2_{\mathrm{s-a}} = 22.9$ if we allow also for QVO. For 3 d.o.f. the $\Delta\chi^2_{\mathrm{s-a}} = 22.9$ implies that pure sterile oscillations are ruled out at 99.996% C.L. compared to the active case. From the figure we obtain the bound

$$\text{solar data}: \quad \eta_{\mathrm{s}} \leq 0.45\,. \tag{3}$$

at 99% C.L. for 1 d.o.f.. A complete table of best fit values of $\Delta m^2_{\mathrm{SOL}}$ and θ_{SOL} with the corresponding χ^2_{SOL} and GOF values for pure active, pure sterile, and mixed neutrino oscillations is given in [5], both for the $\mathrm{SNO}^{\mathrm{rate}}_{\mathrm{CC}}$ $(48-2$ d.o.f.) and the $\mathrm{SNO}^{\mathrm{SP,DN}}_{\mathrm{CC,NC}}$ analysis $(81-2$ d.o.f.).

2. ATMOSPHERIC NEUTRINOS

Here I summarize the analysis of atmospheric data given in Ref. [5], in a generalized oscil-

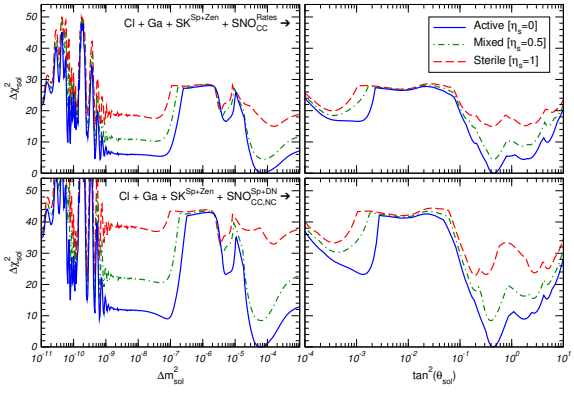

Figure 2. $\Delta\chi^2_{\rm SOL}$ as a function of $\Delta m^2_{\rm SOL}$ and $\tan^2\theta_{\rm SOL}$, for pure active ($\eta_s = 0$), pure sterile ($\eta_s = 1$) and mixed neutrino oscillations ($\eta_s = 0.5$). Upper and lower panels correspond to the $\mathrm{SNO}^{\rm rate}_{\rm CC}$ and $\mathrm{SNO}^{\rm SP,DN}_{\rm CC,NC}$ samples defined in Ref. [5].

lation scheme in which a light sterile neutrino takes part in the oscillations, under the approximation $\Delta m^2_{\rm SOL} \ll \Delta m^2_{\rm ATM}$. In order to comply with the strong constraints from reactor experiments [11] we completely decouple the electron neutrino from atmospheric oscillations. In contrast with the case of solar oscillations, the constraints on the ν_μ–content in atmospheric oscillations are not so stringent. Thus the description of atmospheric neutrino oscillations in this general framework requires two parameters besides the standard 2-neutrino oscillation parameters $\theta_{\rm ATM}$ and $\Delta m^2_{\rm ATM}$. We will use the parameters d_μ and d_s already introduced in Ref. [13], and defined in such a way that $1 - d_\mu$ $(1 - d_s)$ corresponds to the fraction of ν_μ (ν_s) participating in oscillations with $\Delta m^2_{\rm ATM}$. Hence, pure active atmospheric oscillations with $\Delta m^2_{\rm ATM}$ are recovered when $d_\mu = 0$ and $d_s = 1$. In four-neutrino models there is a mass scheme-dependent relationship between d_s and the solar parameter η_s. For details see Ref. [13].

To get a feeling on the physical meaning of these two parameters, note that for $d_\mu = 0$ we obtain that the ν_μ oscillates with $\Delta m^2_{\rm ATM}$ to a linear combination of ν_τ and ν_s given as $\nu_\mu \to \sqrt{d_s}\,\nu_\tau + \sqrt{1-d_s}\,\nu_s$.

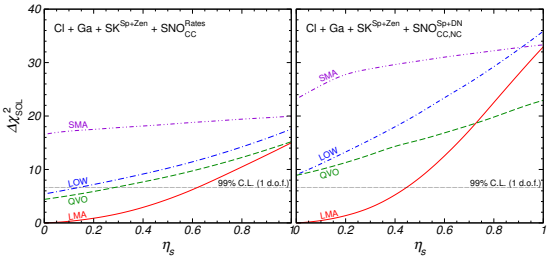

Figure 3. $\Delta\chi^2_{\rm SOL}$ displayed as a function of η_s with respect to favored active LMA solution, for the $\mathrm{SNO}^{\rm rate}_{\rm CC}$ (left panel) and the $\mathrm{SNO}^{\rm SP,DN}_{\rm CC,NC}$ (right panel) analysis, as defined in Ref. [5].

Our global best fit point occurs at

$$\sin^2\theta_{\rm ATM} = 0.49\,, \quad \Delta m^2_{\rm ATM} = 2.1\times 10^{-3}\ \mathrm{eV}^2 \qquad (4)$$

and has $d_s = 0.92$, $d_\mu = 0.04$. We see that atmospheric data prefers a small sterile neutrino admixture. However, this effect is not statistically significant, since the pure active case ($d_s = 1, d_\mu = 0$) also gives an excellent fit: the difference in χ^2 with respect to the best fit point is only $\Delta\chi^2_{\rm act-best} = 3.3$. For the pure active best fit point we obtain,

$$\sin^2\theta_{\rm ATM} = 0.5\,,\ \Delta m^2_{\rm ATM} = 2.5\times 10^{-3}\ \mathrm{eV}^2 \qquad (5)$$

with the 3σ ranges (1 d.o.f.)

$$0.3 \le \sin^2\theta_{\rm ATM} \le 0.7 \qquad (6)$$

$$1.2\times 10^{-3}\ \mathrm{eV}^2 \le \Delta \mathrm{m}^2_{\rm ATM} \le 4.8\times 10^{-3}\ \mathrm{eV}^2\,. \qquad (7)$$

The determination of the parameters $\theta_{\rm ATM}$ and $\Delta m^2_{\rm ATM}$ is summarized in Figs. 4 and 5. Note that Fig. 5 considers several cases: arbitrary d_s and d_μ, best–fit d_s and d_μ, and pure active and mixed active–sterile neutrino oscillations, as indicated.

At a given C.L. we cut the $\chi^2_{\rm ATM}$ at a $\Delta\chi^2$ determined by 4 d.o.f. to obtain 4-dimensional volumes in the parameter space of $(\theta_{\rm ATM}, \Delta m^2_{\rm ATM}, d_\mu, d_s)$. In the upper panels we show sections of these volumes at values of $d_s = 1$ and $d_\mu = 0$ corresponding to the pure active case (left) and the best fit point (right). Again we observe that moving from pure active to the best fit does not change

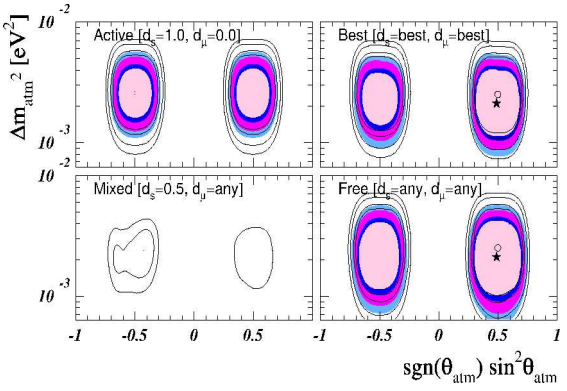

Figure 4. Allowed regions of $\sin^2\theta_{\rm ATM}$ and $\Delta m^2_{\rm ATM}$ at 90%, 95%, 99% and 3σ for 4 d.o.f. and different assumptions on the parameters d_s and d_μ, from [5]. The lines (shaded regions) correspond to 1289 (1489) days of Super-K data.

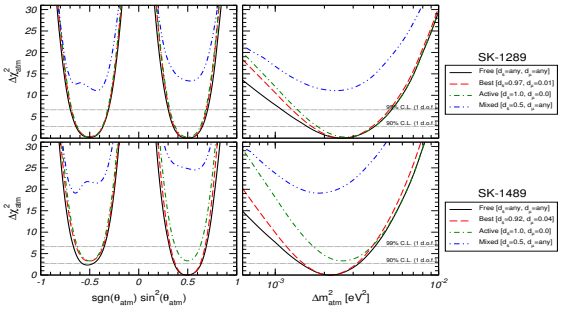

Figure 5. $\Delta\chi^2_{\rm ATM}$ as a function of $\sin^2\theta_{\rm ATM}$ (left) and $\Delta m^2_{\rm ATM}$ (right), using 1289 (upper) and 1489 (lower) days of Super-K data [5].

the fit significantly. In the lower right panel we project away both d_μ and d_s, whereas in the lower left panel we fix $d_s = 0.5$ and eliminate only d_μ. Comparing the regions resulting from 1489 days Super-K data (shaded regions) with the one from the 1289 days Super-K sample (hollow regions) we note that the new data leads to a slightly better determination of $\theta_{\rm ATM}$ and $\Delta m^2_{\rm ATM}$. However, more importantly, from the lower left panel we see, that the new data shows a much stronger rejection against a sterile admixture: for $d_s = 0.5$ no allowed region appears at 3σ for 4 d.o.f..

3. NEUTRINO PARAMETERS

The basic structure of the neutrino sector required to account for present solar and atmospheric data has been developed in the early eighties, motivated mainly by theory [14, 15, 16, 17]. In a gauge theory of the weak interaction the `simplest` lepton mixing matrix is characterized by 3 angles and 3 CP violating phases [18]:

- the solar angle θ_{12}
- the atmospheric angle θ_{23}
- the reactor angle θ_{13}
- one Kobayashi-Maskawa-like CP phase
- 2 extra (Majorana-type) CP phases

The structure of leptonic weak interactions is more complex in theories containing $SU(2)\otimes U(1)$ singlet leptons [18], especially if, for some symmetry reason, they happen to be light. In such case the charged current mixing matrix is rectangular and the neutral current is non-trivial, with yet new angles and phases present (see [18] for a detailed discussion and parametrization).

As seen above [19], current solar and atmospheric data fit very well with oscillations among the three active neutrinos, provided that θ_{12} is large as seen in Eq. (2), but non-maximal, given in Eq. (1), while θ_{23} must be nearly maximal, from Eq. (5). As mentioned, θ_{13} must be rather small [12]. Note from Eqs. (2) and (5) that $\Delta m^2_{\rm ATM} \gg \Delta m^2_{\rm SOL}$. Depending on the sign of Δm^2_{32} there are two possible neutrino mass schemes: normal and inverse-hierarchical neutrino masses.

If solar and atmospheric data are combined with short baseline data including the LSND hint, then one needs, in the framework of the oscillation hypothesis, the existence of a light sterile neutrino [9] taking part in the oscillations [13].

With the latest data one finds that, even though 4-neutrino models can not be ruled out as such, the resulting global fit of all current oscillation data is extremely poor [20].

The large solar mixing indicated by present data will lead to significant deformation of the

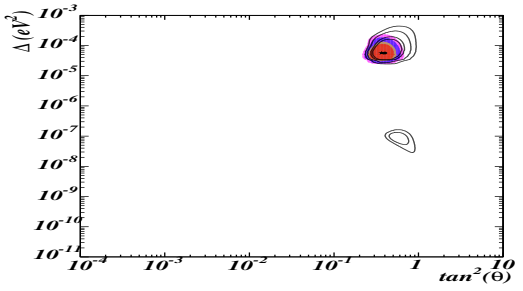

Figure 6. LMA as best solar + SN-1987A fit [22]

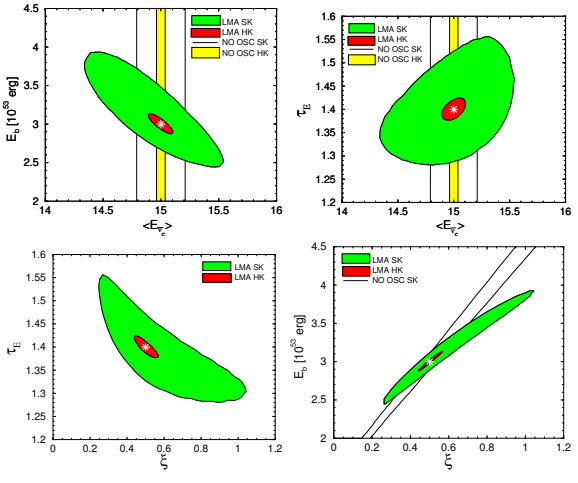

Figure 7. Extracting supernova parameters from LMA oscillations [23]

energy spectra of supernova neutrinos, affecting the resulting signal [21]. However, a global analysis shows that the LMA–MSW may remain as the best solution even after combining SN1987 with solar neutrino data [22]. Finally we note that solar neutrino oscillations with large mixing may allow us in the future to obtain otherwise inaccessible features of SN neutrino spectra. Fig. 7 from [23] shows how one can determine temperatures and luminosities of non-electron flavor neutrinos by observing $\bar{\nu}_e$ from a galactic supernova in massive water Cherenkov detectors using the CC reactions on protons, especially at a Hyper-K–type detector.

Last, but not least, note that neutrino oscillations are sensitive only to mass splittings, not to the absolute scale of neutrino mass, nor to whether neutrinos are Dirac or Majorana particles. The main process relevant to decide this fundamental issue is $\beta\beta_{0\nu}$ decay [24]. The `black-box theorem` states that, in a "natural" gauge theory, irrespective of how $\beta\beta_{0\nu}$ is engendered, it implies a Majorana neutrino mass, and vice-versa, as illustrated by Fig. 8. One may quantify the

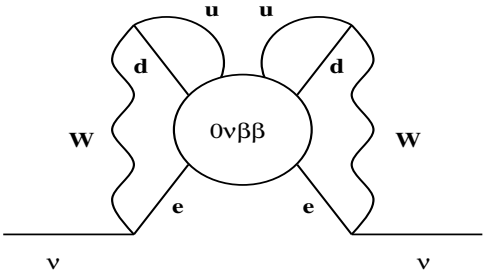

Figure 8. The black-box $\beta\beta_{0\nu}$ argument [25].

implications of the black-box argument once a particular model is specified. The strength of neutrino-exchange-induced $\beta\beta_{0\nu}$ is characterized by an "effective" neutrino mass parameter M_{ee} which takes into account possible cancellations among individual neutrino amplitudes [26, 27]. As seen in Fig. 9 this is directly correlated [28] with the neutrino mass scales probed in tritium beta decays [29] and cosmology [30]. It is therefore important to probe $\beta\beta_{0\nu}$ in a more sensitive experiment, such as GENIUS [31]. Moreover

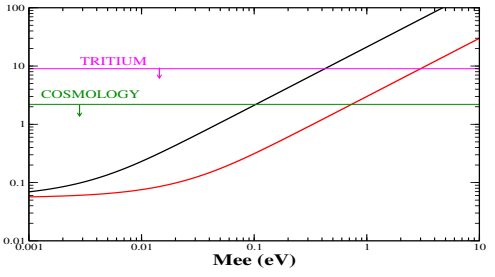

Figure 9. $\beta\beta_{0\nu}$ and the scale of neutrino mass.

$\Delta L = 2$ processes, such as $\beta\beta_{0\nu}$ decay, are sensitive to the "Majorana-type" phases [18, 32] which

drop out from ordinary ($\Delta L = 0$) neutrino oscillations. However it is unlikely that these phases can ever be reliably extracted from $\beta\beta_{0\nu}$ alone. The CP violation induced by the "Dirac" phase is very hard to probe in oscillations, since it disappears as two neutrinos become degenerate [33] and as $\theta_{13} \to 0$ [11]. Fortunately the LMA solution helps, so with good luck, neutrino factories may probe leptonic CP violating effects, through the measurement of CP asymmetries [34].

4. NEUTRINO THEORIES

Basic uncertainties hinder the prediction of neutrino masses from first principles [35]: no knowledge of the underlying scale (the scale of gravity/strings? the GUT scale? an intermediate left-right scale? the weak interaction scale itself?), no knowledge of the underlying mechanism (tree level? radiative? hybrid?) and, last but not least, lack of a theory of flavor, which makes it especially difficult to make an honest prediction of mixing angles. Nevertheless there has been an explosion of models in the last few years, most of which based on the so-called seesaw scheme [15, 16].

An interesting of feature of such seesaw models is that the amount of lepton asymmetry produced in the early universe by the out–of–thermal–equilibrium decay of the right-handed neutrino may be enough to explain the current baryon-to-photon ratio of the Universe [36]. This asymmetry arises from leptonic CP violation associated to the Majorana nature of neutrinos [18].

Various Yukawa textures and gauge groups have been proposed in order to "predict" neutrino mixing angles in the seesaw approach, as described by King [37]. Here I simply mention a few models from our own crop. They fall into two classes: `top-down` and `bottom-up`, and cover both `hierarchical` and `quasi-degenerate` neutrino mass spectra.

The simplest way to give neutrino masses makes use of the basic dimension-5 operator in Fig. 10, first noted by Weinberg [14] whose coefficient is unknown. Since gravity is believed to break global symmetries, such as lepton number, it may induce this operator. Alternatively it may

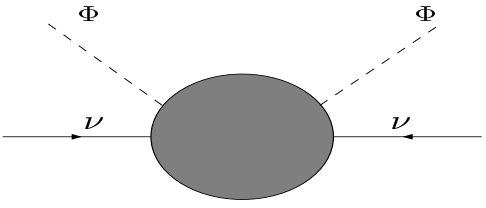

Figure 10. Dimension-5 neutrino mass operator

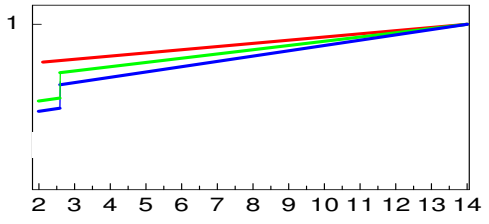

Figure 11. Neutrino masses unifying at 10^{14} GeV

arise from physics at some Grand-unified or intermediate scale, `a la seesaw`. A radical idea [38] is that, due to some symmetry, valid at some high-energy scale M_X, neutrino masses "unify" at that scale, as indicated in Fig. 11. Such a simple ansatz naturally leads to quasi-degenerate neutrinos at low scales, which could lie in the electron-volt range, while the tiny solar and atmospheric neutrino mass splittings are induced by renormalization effects. An interesting choice for the underlying symmetry is the discrete non-Abelian symmetry A_4 [39], which can be realized without spoiling the hierarchy of charged-lepton masses. Solar and atmospheric neutrino mass splittings, maximal atmospheric and large solar mixings are then induced radiatively in softly broken supersymmetry. The quark mixing matrix is also calculable in a similar way. The mixing parameter U_{e3} is predicted to be small and imaginary, leading to maximal CP violation in neutrino oscillations. The ν_e is a Majorana neutrino while the muon and tau neutrinos form a pseudo-Dirac pair [26]. We found that $\beta\beta_{0\nu}$ and $\tau \to \mu\gamma$ decay rates fall in the experimentally accessible range.

Another minimalistic way to generate neutrino mass and mixings has been suggested in [40]. It consists in producing the atmospheric neutrino scale `a la seesaw` with just one $SU(3)\otimes SU(2)\otimes U(1)$ singlet lepton [18, 33]. In this approximation two of the neutrinos are massless, their degeneracy being lifted by the gravitationally induced dimension-5 operator discussed above. The required neutrino parameters can be easily accommodated. Since the solar scale comes from Planck-mass effects, the solar neutrino problem is explained by vacuum oscillations, which may be tested through the search for anomalous seasonal effects at Borexino.

I now turn to the possibility that neutrino masses may have an intrinsically supersymmetric origin, through the breaking of R–parity [41, 42, 43]. I focus on the bilinear violation of R–parity [44, 45], described by

$$W = W_{\rm MSSM} + \epsilon_a \ell_a H_u \tag{8}$$

where $W_{\rm MSSM}$ is the MSSM superpotential, ϵ_a ($a = e, \mu, \tau$) denote the strength of bilinear terms involving the lepton (ℓ_a) and up-type Higgs (H_u) superfields. The bilinear terms lead to `one` tree level neutrino mass, chosen to lie in the range required by the atmospheric neutrino data, while calculable radiative contributions lift the degeneracy of the other neutrinos giving rise to the solar neutrino scale [46].

This provides the simplest, most predictive and systematic effective R–parity violation model at low–energies. Its theoretical basis can be found either in the context of models where R–parity breaking is introduced explicitly `ab initio` [42], or in models where the violation of R–parity occurs `spontaneously`, through a nonzero $SU(2)\otimes U(1)$ singlet sneutrino vacuum expectation value [43].

A recent example of the former kind was given in [47] using an anomalous U(1) horizontal symmetry which forbids all trilinear R-parity violating superpotential terms, selecting only the bilinear ones, and relating their strength ϵ_a to powers of the U(1) breaking parameter $\theta \sim 0.22$. This gives a common origin for the μ–term related to electroweak breaking and for the L-violating terms generating neutrino masses. The latter are suitable for explaining neutrino anomalies, though radiative contributions prefer the presently disfavored QVO solutions to the solar neutrino problem. This can be tested through the search for anomalous seasonal effects. The neutrino mixing angles are not suppressed by powers of θ and can naturally be large.

Spontaneous R–parity breaking models require the addition of $SU(2)\otimes U(1)$ singlet superfields, e. g. right-handed neutrinos, and give a dynamical origin for the bilinear strength ϵ_a identified as $\epsilon_a = h_{\nu ab} v_{Rb}$ where $h_{\nu ab}$ is the Dirac Yukawa matrix. A characteristic feature of these models is the existence of an novel variant (L=1) of the singlet seesaw majoron [17]. Majoron emission induces "invisible" neutrino [17] and Higgs boson decays [48]. The former are relevant in astrophysical environments [49], while the latter lead to sizable Higgs–to–missing–transverse–momentum signals [50].

In addition to explaining neutrino anomalies, supersymmetry with bilinear breaking of R–parity leads to a variety of phenomenological implications [51]. Some examples are: unification predictions for gauge and Yukawa couplings, $m_{\rm top}$, V_{cb} and $\tan\beta$ [52, 53, 54], $b \to s\gamma$ [55], $\beta\beta_{0\nu}$ [56], charged and neutral Higgs boson decays [57], top quark decays [58], chargino [59] and neutralino decays [60], and gluino cascade decays [61]. Barring fine-tuning or other assumptions, the smallness of the neutrino masses suppresses many of these effects in the most generic bilinear model of neutrino anomalies. However, there is at least one which survives and which may lead to a dramatic confirmation of the neutrino anomalies at high energy accelerator experiments such as the LHC or NLC: the decays of the lightest supersymmetric particle (LSP). This is a very striking feature of the model which holds irrespective of what is the nature of the LSP. We have considered the cases of lightest neutralino as LSP [62], lightest stop as LSP [63] and lightest stau as LSP [64]. As an example, the left panel in Fig. 12 shows the LSP decay length in cm versus mass in GeV, when it is the lightest neutralino. On the other hand the right panel gives the ratio of predicted LSP decay semileptonic decay branching ratios to muons over taus

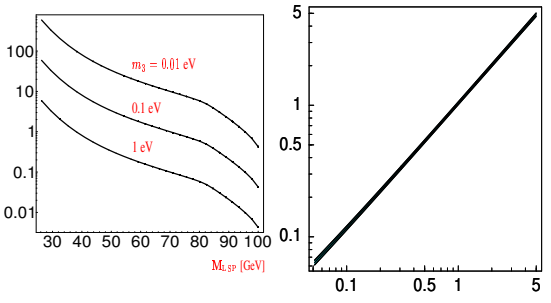

Figure 12. LSP decay length [60] and predicted semileptonic decay branching ratios [62].

(ordinate) versus the atmospheric neutrino mixing angle (abscissa), illustrating a perfect correlation: if $\theta_{\rm ATM} = \pi/4$ one expects equal numbers of muons and taus in semileptonic neutralino decays. Similarly, the solar and reactor neutrino angles can be probed in various LSP decay scenarios, see [62, 63, 64] for details.

5. NON-STANDARD NEUTRINOS

Non-standard neutrinos interactions (NSI) are expected in most neutrino mass models [18, 35] and can be of two types: flavour-changing (FC) and non-universal (NU). They may arise from a nontrivial structure of CC and NC weak interactions characterized a non-unitary lepton mixing matrix and a correspondingly non-trivial NC matrix [18]. Such `gauge-induced` NSI may lead to flavor and CP violation, even with degenerate massless neutrinos [65]. In radiative models of neutrino mass [66] and supersymmetric models with broken R parity [41, 42] FC-NSI can also be `Yukawa-induced`, from the exchange of spinless bosons. In supersymmetric unified models, they may be calculable as renormalization effects [67].

At the moment one can not yet pin down the exact profile of the ν_e survival probability and, as a result, the underlying mechanism of solar neutrino conversion remains unknown. Alternatives to oscillations have been suggested since the eighties, including non-standard neutrino matter interactions (NSI) [68] and spin-flavor precession (SFP) [69, 70]. The former may be represented as effective dimension-6 terms of the type εG_F, as illustrated in Fig. 13, where ε specifies their sub-weak strength.

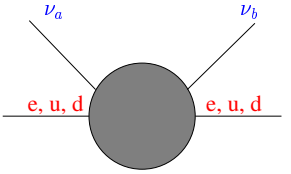

Figure 13. Effective NSI operator.

Analyses of solar neutrino data in terms of NSI [71] and SFP [72, 73, 74] have been given recently. SFP solutions exist both in the resonant (RSFP) [74] and non-resonant regimes (NRSFP) [73]. The NSI solar neutrino energy spectrum is undistorted, in agreement with data. On the other hand Fig. 14 shows the predicted modification of the solar neutrino spectra for the "best" LMA solution, and for the "best" SFP solutions [72], from latest solar data. Clearly the spectra in the high energy region are nearly undistorted in all 3 cases, in agreement with observations.

Although LMA oscillations are clearly favored over other `oscillation` solutions [5, 6], present solar neutrino data `can be equally well--described by SFP and NSI solutions`. Fig. 15 shows that this is indeed the case, the resulting parameter regions is given in Fig. 16. Although all 3 solutions are statistically equivalent, one sees that that the two SFP solutions lie slightly lower than the LMA minimum. Note that in the presence of a neutrino transition magnetic moment of 10^{-11} Bohr magneton, a magnetic field of 80 KGauss eliminates all oscillation solutions other than LMA. Ways to separate these 3 solutions at Borexino have been considered in [72, 75].

Similarly the regions for the NSI mechanism are shown in Fig. 17. The required NSI values indicated by the solar data analysis are fully acceptable also for the atmospheric data. Such NSI description of solar data was also shown [71] to be slightly better than that of the LMA oscillation solution.

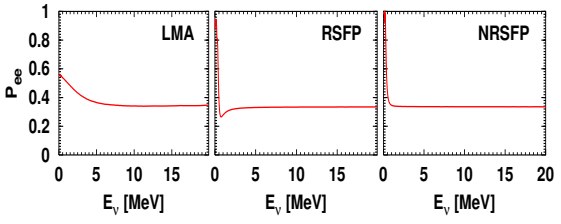

Figure 14. Best LMA and SFP ν_e survival probabilities from [72]

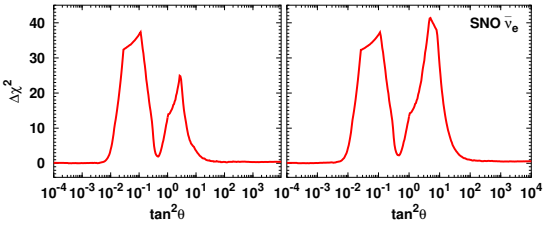

Figure 15. $\Delta\chi^2_{\rm SOL}$ versus $\tan^2\theta_{\rm SOL}$, for RSFP, LMA (central minima) and NRSFP solutions. Left and right panels refer to two different analyses described in Ref. [72].

Can NSI play a role in the atmospheric neutrino signal? FC-NSI interactions in the ν_μ - ν_τ channel without neutrino mass nor mixing have been shown to account for the zenith–angle–dependent deficit of atmospheric neutrinos observed in `contained` Super-K events [76, 77]. However such NSI explanation fails to reconcile these with Super-K and MACRO `up-going muons`, due to the lack of energy dependence intrinsic of NSI conversions. As a result, a pure NSI conversion in the atmospheric channel is ruled out at 99% C.L. [78]. Thus, unlike the case of solar neutrinos, the oscillation interpretation of atmospheric data is robust, NSI being allowed only at a sub-leading level. Such robustness of the atmospheric $\nu_\mu \to \nu_\tau$ oscillation hypothesis can be used to provide the most stringent present limits on FC and NU neutrino interactions, as illustrated in Fig. 18. These limits are also the most model–independent, as they are obtained from pure neutrino-physics processes.

Future neutrino factories aim at probing the

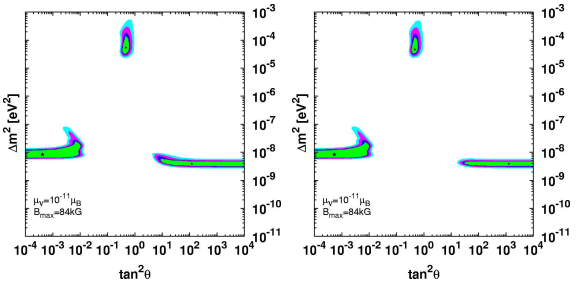

Figure 16. Allowed $\Delta m^2_{\rm SOL}$ and $\tan^2\theta_{\rm SOL}$ for RSFP, LMA and NRSFP solutions for the indicated values of μB, from [72]

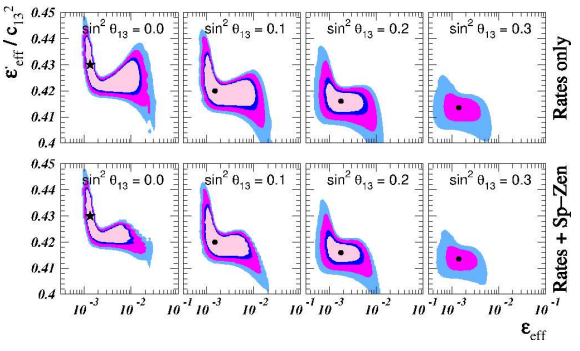

Figure 17. Parameters of NSI solution to the solar neutrino anomaly, from [71].

lepton mixing angle θ_{13} with much better sensitivity than possible at present [34]. They may also probe NSI in the ν_μ -ν_τ channel [79], with substantially improved sensitivity in the case of FC-NSI, especially at energies higher than approximately 50 GeV. For example, a 100 GeV `Nufact` can probe FC-NSI interactions at the level of $|\epsilon| <$ few $\times 10^{-4}$ at 99 % C.L.

Note also that in such hybrid solution to the neutrino anomalies, with FC-NSI explaining the solar data, and oscillations accounting for the atmospheric data, the two sectors are connected not only by the neutrino mixing angle θ_{13}, but also by the ν_e -ν_τ FC-NSI parameters. As a result NSI and oscillations may be confused, as shown in [80]. This implies that information on θ_{13} can only be obtained if bounds on NSI are available.

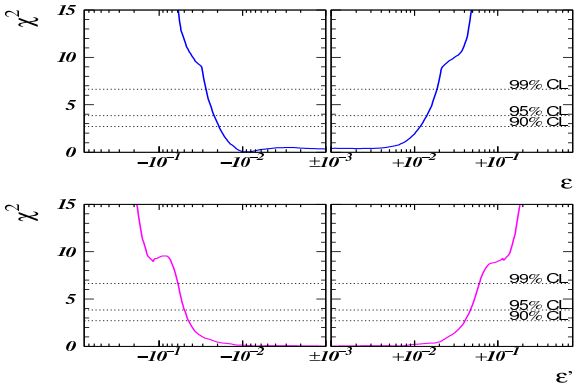

Figure 18. Atmospheric bounds on NSI [78].

Taking into account the existing bounds on FC interactions, one finds a drastic loss in `Nufact` sensitivities on θ_{13}, of at least two orders of magnitude. A near–detector offers the possibility to obtain stringent bounds on some NSI parameters and therefore constitutes a crucial necessary step towards the determination of θ_{13} and subsequent study of leptonic CP violation.

Last, but not least, note that the KamLAND experiment [81] will provide vital information very soon. Even if the LMA solution is finally confirmed by KamLAND, such alternative mechanisms will still be interesting for study since their sub-leading admixture may be testable, as discussed in [72, 82]. They may also affect the propagation of neutrinos in a variety of astrophysical environments [83].

References

[1] Talks by T. Kirsten, V. Gavrin, K. Lande.

[2] M. Smy, these proceedings.

[3] A. Hallin, these proceedings.

[4] J. Bahcall, these proceedings.

[5] M. Maltoni, T. Schwetz, M. A. Tortola and J. W. Valle, arXiv:hep-ph/0207227.

[6] Talks by A. Smirnov and E. Lisi.

[7] L. Wolfenstein, Phys. Rev. D **17**, 2369 (1978); S. P. Mikheev and A. Y. Smirnov, Sov. J. Nucl. Phys. **42** (1985) 913

[8] M. C. Gonzalez-Garcia, P. C. de Holanda, C. Pena-Garay and J. W. Valle, Nucl. Phys. B **573**, 3 (2000)

[9] J. T. Peltoniemi, D. Tommasini and J. W. Valle, Phys. Lett. B **298**, 383 (1993). J. T. Peltoniemi and J. W. Valle, Nucl. Phys. B **406**, 409 (1993); D. O. Caldwell and R. N. Mohapatra, Phys. Rev. D **48** (1993) 325; additional references in Giunti and Lavader's excellent web–page http://www.to.infn.it/ giunti/neutrino/

[10] G. Drexlin, these proceedings.

[11] M. Apollonio et al, CHOOZ Coll., Phys. Lett. B **466** (1999) 415; F. Boehm et al, Palo Verde Coll., Phys. Rev. D **64** (2001) 112001

[12] M. C. Gonzalez-Garcia, M. Maltoni, C. Pena-Garay and J. W. Valle, Phys. Rev. D **63**, 033005 (2001)

[13] M. Maltoni, T. Schwetz and J. W. Valle, Phys. Rev. D **65**, 093004 (2002); Phys. Lett. B **518** (2001) 252

[14] S. Weinberg, Proceedings of `Neutrinos 78`, p, 1-21; R. Barbieri, J. R. Ellis and M. K. Gaillard, Phys. Lett. B **90**, 249 (1980).

[15] M. Gell-Mann, P. Ramond and R. Slansky in *Supergravity* (North Holland, Amsterdam 1979); T. Yanagida in *Proc. of the Workshop on Unified Theory and Baryon Number of the Universe*, KEK, Japan, 1979.

[16] R. N. Mohapatra and G. Senjanovic, Phys. Rev. Lett. **44** (1980) 912; J. Schechter and J. W. Valle, Phys. Rev. D **22**, 2227 (1980); C. Wetterich, Nucl. Phys. B **187** (1981) 343.

[17] Y. Chikashige, R. N. Mohapatra and R. D. Peccei, Phys. Lett. B **98** (1981) 265; J. Schechter and J. W. Valle, Phys. Rev. D **25** (1982) 774; G. B. Gelmini and J. W. Valle, Phys. Lett. B **142**, 181 (1984).

[18] J. Schechter and J. W. Valle, Phys. Rev. D **22**, 2227 (1980); Phys. Rev. D **23**, 1666 (1981).

[19] For a phenomenological review see S. M. Bilenky, C. Giunti and W. Grimus, Prog. Part. Nucl. Phys. **43** (1999) 1

[20] M. Maltoni, T. Schwetz, M. A. Tortola and J. W. Valle, arXiv:hep-ph/0207157.

[21] A. Y. Smirnov et al, Phys. Rev. D **49** (1994) 1389; B. Jegerlehner, F. Neubig and G. Raffelt, Phys. Rev. D **54**, 1194 (1996); M. Kachelriess et al, JHEP **0101**, 030 (2001)

[22] M. Kachelriess, A. Strumia, R. Tomas and J. W. Valle, Phys. Rev. D **65**, 073016 (2002)

[23] H. Minakata, H. Nunokawa, R. Tomas and J. W. Valle, Phys. Lett. B **542**, 239 (2002)

[24] A. Morales, Nucl. Phys. Proc. Suppl. **77**, 335 (1999); A. Faessler and F. Simkovic, Prog. Part. Nucl. Phys. **46** (2001) 233.

[25] J. Schechter and J. W. Valle, Phys. Rev. D **25**, 2951 (1982).

[26] L. Wolfenstein, Nucl. Phys. B **186** (1981) 147. J. W. Valle and M. Singer, Phys. Rev. D **28**, 540 (1983).

[27] J. W. Valle, Phys. Rev. D **27**, 1672 (1983).

[28] V. Barger et al, Phys. Lett. B **532** (2002) 15. F. Feruglio, A. Strumia and F. Vissani, arXiv:hep-ph/0201291; H. Minakata and H. Sugiyama, Phys. Lett. B **532**, 275 (2002)

[29] Ch. Weinheimer, these proceedings.

[30] O. Elgaroy et al, arXiv:astro-ph/0204152.

[31] H. V. Klapdor-Kleingrothaus et al, [GENIUS Collaboration], arXiv:hep-ph/9910205.

[32] M. Doi, T. Kotani and E. Takasugi, Prog. Theor. Phys. Suppl. **83**, 1 (1985).

[33] J. Schechter and J. W. Valle, Phys. Rev. D **21**, 309 (1980).

[34] Talks by F. Dydak, S. Geer and M. Lindner.

[35] J. W. Valle, Prog. Part. Nucl. Phys. **26**, 91 (1991).

[36] T. Yanagida, these proceedings.

[37] S. F. King, these proceedings.

[38] P. H. Chankowski et al, Phys. Rev. Lett. **86** (2001) 3488

[39] K. S. Babu, E. Ma and J. W. Valle, arXiv:hep-ph/0206292.

[40] A. de Gouvea and J. W. Valle, Phys. Lett. B **501**, 115 (2001)

[41] C. S. Aulakh and R. N. Mohapatra, Phys. Lett. B **119** (1982) 13; G. G. Ross and J. W. F. Valle, Phys. Lett. B **151** (1985) 375; J. R. Ellis et al, Phys. Lett. B **150** (1985) 142; A. Santamaria and J. W. F. Valle, Phys. Lett. B **195**, 423 (1987); Phys. Rev. Lett. **60**, 397 (1988); Phys. Rev. D **39**, 1780 (1989).

[42] L. J. Hall and M. Suzuki, Nucl. Phys. B **231** (1984) 419, see also [51] and papers therein.

[43] A. Masiero and J. W. F. Valle, Phys. Lett. B **251** (1990) 273; J. C. Romao et al, Phys. Lett. B **288** (1992) 311. J. C. Romao and J. W. F. Valle, Nucl. Phys. B **381** (1992) 87

[44] J. W. Valle, Proceedings of 6th Int. Symposium on Particles, Strings and Cosmology (PASCOS 98), p. 502-512; arXiv:hep-ph/9808292 and references therein.

[45] M. A. Diaz, J. C. Romao and J. W. Valle, Nucl. Phys. B **524**, 23 (1998)

[46] M. Hirsch et al, Phys. Rev. D **62**, 113008 (2000) [Err.-ibid. D **65**, 119901 (2002)]; J. C. Romao et al, Phys. Rev. D **61**, 071703 (2000)

[47] J. M. Mira et al, Phys. Lett. B **492**, 81 (2000)

[48] J. C. Romao, F. de Campos and J. W. Valle, Phys. Lett. B **292**, 329 (1992) A. S. Joshipura and J. W. Valle, Nucl. Phys. B **397** (1993) 105

[49] M. Kachelriess, R. Tomas and J. W. Valle, Phys. Rev. D **62** (2000) 023004

[50] M. Carena et al, "Higgs physics", Report of the Workshop on Physics at LEP2, ed. G. Altarelli et al, arXiv:hep-ph/9602250. F. de Campos et al, Phys. Rev. D **55** (1997) 1316; M. A. Diaz et al, Nucl. Phys. B **527**, 44 (1998); Phys. Rev. D **58**, 057702 (1998)

[51] B. Allanach et al, arXiv:hep-ph/9906224.

[52] M. A. Diaz, J. Ferrandis and J. W. Valle, Nucl. Phys. B **573**, 75 (2000)

[53] M. A. Diaz et al, Nucl. Phys. B **590**, 3 (2000)

[54] M. A. Diaz et al, Phys. Lett. B **453**, 263 (1999)

[55] M. A. Diaz et al, Nucl. Phys. B **551**, 78 (1999)

[56] M. Hirsch et al, Phys. Lett. B **486**, 255 (2000); M. Hirsch and J. W. Valle, Nucl. Phys. B **557**, 60 (1999)

[57] A. G. Akeroyd et al, Nucl. Phys. B **529**, 3 (1998); F. de Campos et al, Nucl. Phys. B **451**, 3 (1995)

[58] L. Navarro, W. Porod and J. W. Valle, Phys. Lett. B **459**, 615 (1999)

[59] F. de Campos et al, Nucl. Phys. B **546**, 33 (1999)

[60] A. Bartl et al, Nucl. Phys. B **600**, 39 (2001)

[61] A. Bartl et al, Nucl. Phys. B **502**, 19 (1997)

[62] W. Porod et al, Phys. Rev. D **63**, 115004 (2001)

[63] D. Restrepo et al, Phys. Rev. D **64**, 055011 (2001); M. A. Diaz et al, Nucl. Phys. B **583**, 182 (2000)

[64] M. Hirsch et al, arXiv:hep-ph/0207334.

[65] R. N. Mohapatra and J. W. F. Valle, Phys. Rev. D **34** (1986) 1642. D. Wyler and L. Wolfenstein, Nucl. Phys. B **218** (1983) 205.

[66] A. Zee, Phys. Lett. B **93** (1980) 389 [Err-ibid. B **95** (1980) 461]. K. S. Babu, Phys. Lett. B **203** (1988) 132.

[67] L. J. Hall, V. A. Kostelecky and S. Raby, Nucl. Phys. B **267** (1986) 415 R. Barbieri, L. J. Hall and A. Strumia, Nucl. Phys. B **445**, 219 (1995) F. Gabbiani et al, Nucl. Phys. B **477**, 321 (1996)

[68] J. W. Valle, Phys. Lett. B **199**, 432 (1987).

[69] E. K. Akhmedov, Phys. Lett. B **213** (1988) 64. C. S. Lim and W. J. Marciano, Phys. Rev. D **37** (1988) 1368.

[70] J. Schechter and J. W. Valle, Phys. Rev. D **24**, 1883 (1981) [Err.-ibid. D **25**, 283 (1982)].

[71] M. Guzzo et al, Nucl. Phys. B **629**, 479 (2002)

[72] J. Barranco et al, arXiv:hep-ph/0207326.

[73] O. G. Miranda et al, Phys. Lett. B **521**, 299 (2001)

[74] O. G. Miranda et al, Nucl. Phys. B **595**, 360 (2001)

[75] E. K. Akhmedov and J. Pulido, Phys. Lett. B **529**, 193 (2002)

[76] N. Fornengo et al, JHEP **0007**, 006 (2000)

[77] M. C. Gonzalez-Garcia et al, Phys. Rev. Lett. **82**, 3202 (1999)

[78] N. Fornengo et al, Phys. Rev. D **65**, 013010 (2002)

[79] P. Huber and J. W. Valle, Phys. Lett. B **523**, 151 (2001)

[80] P. Huber, T. Schwetz and J. W. Valle, Phys. Rev. Lett. **88**, 101804 (2002) and Phys. Rev. D **66**, 013006 (2002)

[81] J. Shirai, these proceedings.

[82] W. Grimus et al, arXiv:hep-ph/0208132.

[83] H. Nunokawa et al, Phys. Rev. D **54**, 4356 (1996); H. Nunokawa et al, Nucl. Phys. B **482**, 481 (1996); D. Grasso et al, Phys. Rev. Lett. **81**, 2412 (1998); G. L. Fogli et al, Phys. Rev. D **66**, 013009 (2002)